

ESTIMATION OF GROUND REACTION FORCES FROM MARKERLESS KINEMATICS AND COMPARISON AGAINST MEASURED FORCE PLATE DATA

Steffi Colyer^{1,2}, Laurie Needham^{1,2,3}, Murray Evans^{1,4}, Logan Wade^{1,2}, Darren Cosker^{1,4}, Dario Cazzola^{1,2}, Polly McGuigan^{1,2} and James Bilzon^{1,2}

Centre for the Analysis of Motion, Entertainment Research and Applications,
University of Bath, UK¹
Department of Health, University of Bath, UK²
Seiko Timing Systems, UK³
Department of Computer Science, University of Bath, UK⁴

This study investigated how accurately ground reaction forces (GRFs) can be estimated from body centre of mass (BCOM) motion derived using markerless motion capture. Fifteen participants performed a countermovement jump (CMJ) on, and a running trial across, force plates. Kinematics captured using markerless and marker-based systems were used to drive IK-constrained OpenSim models. The resulting BCOM displacements were double differentiated to inversely estimate GRFs and compared to force plate data. Markerless-derived estimates were similar to measured GRFs (RMSD = ~70-150 N) and vertical peak force, impulse and rate of force development were also accurately estimated (effect sizes < 0.2), similarly to marker-based outputs. Our markerless workflow shows promise for the estimation of vertical GRF parameters out in the field, without markers or force plates.

KEYWORDS: computer vision, inverse approach, validation.

INTRODUCTION: Ground reaction force (GRF) production is a fundamental biomechanical measure, with GRF parameters associated with performance (Morin et al. 2012) and musculoskeletal injury (Johnson et al. 2020). Additionally, GRFs underpin the biomechanical load experienced by an athlete and thus are also important from a training load monitoring perspective. Ultimately, however, a biomechanist's desire to measure GRFs stems from the mechanical fact that external forces directly cause the observed motion. Thus, we can, for example, compute the body centre of mass (BCOM) motion using a forward dynamics approach (from GRFs) or compute the GRFs required to generate the BCOM motion using an inverse approach (from whole-body kinematics and segmental modelling).

In certain cases, however, collecting GRFs is not possible and, even when force plates are available, researchers and practitioners may be limited to collect only a small number of gait cycles, for example. Thus, the potential to utilise an inverse approach to estimate GRFs from 3D marker-derived kinematics has been explored previously, allowing some relevant GRF parameters (e.g. vertical impulse) to be computed during running (Pavei et al. 2017). However, marker-based methods are also restricted to certain (often laboratory-based) settings and the participant preparation time (particularly for whole-body 3D kinematics) can make this analysis unfeasible in certain situations, not least when investigating elite athletes.

Markerless motion capture has opened up the possibility to collect whole-body kinematics outside of the laboratory with minimal participant interference, and this shows great promise in terms of the validity of certain joint kinematic outputs (Needham et al. 2022). However, it is currently unknown how accurately GRFs can be estimated from the markerless-derived BCOM motion alone. Thus, the purpose of this study was to estimate GRFs during running and countermovement jumping (CMJ) using BCOM motion (inversely) computed from marker-based and markerless motion capture, and compare these outputs against measured GRFs.

METHODS: Fifteen participants (7 males, 8 females [1.71 ± 0.10 m, 73.7 ± 14.7 kg]) provided written informed consent to participate. Each participant performed a running trial across the laboratory at a self-selected speed and a maximal-effort CMJ. Four force plates (Kistler 9287BA; 1000 Hz) embedded in the laboratory floor were used to capture the GRFs produced

across the entire CMJ trial and at least one ground contact during the running trials. Motion data were captured synchronously (at 200 Hz) using markerless (9 JAI machine-vision cameras; JAI sp5000c) and marker-based (15 Oqus Qualisys cameras) systems. A binary circle pattern board was used to calibrate the markerless system, whereas a wand calibration was used for the marker-based system. The Qualisys L-frame was placed in the centre of the capture volume and a single marker was randomly moved and tracked in both systems through the space to allow spatial alignment. Full methodological details can be found elsewhere (Needham et al. 2022). Briefly, OpenPose (Cao et al. 2017; 'body_25' model) was applied to each 2D markerless camera view to provide 25 sparse keypoints. These were then fused to reconstruct the 3D joint centres before being passed through a bi-directional Kalman filter. A full-body marker set (44 individual markers and four clusters) allowed bilateral feet, shanks and thighs, pelvis and thorax, upper and lower arms, and hands to be tracked. Marker trajectories were then gap-filled in Qualisys Track Manager (v2019.3) and exported, before being filtered with a low-pass Butterworth filter with 12-Hz cut-off frequency.

The outputs for both markerless and marker-based systems were used to drive the motion of a constrained OpenSim model. For each participant, a linearly-scaled model was produced for the markerless and marker-based data separately, before the model pose was globally optimised in each frame using the OpenSim Inverse Kinematics (IK) tool (equal weighting across landmarks, except shoulder and toe markers). The hip joints were modelled as 3 DoF, the knee joints as 1DoF (flexion/extension) and the ankle joint as 2DoF (plantar dorsi/plantar flexion and ankle ad/abduction) joints. The BCOM positions (weighted sum of segmental centre of mass locations, according to the 'Gait2354' model; Delp et al. 1990) in the vertical (all trials) and horizontal (running trials only) direction were then extracted from the IK skeletal model. This positional information was double differentiated to calculate BCOM acceleration in the same directions as above, before being multiplied by the participant's mass to provide an estimated GRF. In the vertical direction, the participant's weight was also added.

The estimated GRFs were then compared against the measured GRF (force plates) across the whole CMJ movement and across the ground contact phase of the running trials (identified using a 20-N vertical-force threshold). A root mean squared difference (RMSD) in force was calculated across the phase of interest for marker-based and markerless systems. To directly compare and visualise the estimated and measured GRFs, these data were time-normalised to 101 nodes. Several discrete force parameters were also calculated including peak forces, net impulses (time integral of force), rate of force development during CMJ (RFD; average slope from the start of active force production to the peak vertical force) and loading rate during running (average slope from 25-75% of the initial vertical GRF peak). Differences between the estimated force parameters and those measured via the force plate were evaluated using effect sizes (ESs; Cohen's *d*) and 90% confidence intervals (CIs). Differences were considered to be clear and non-trivial if an ES was greater than 0.2 (or less than -0.2) and the 90% CI did not overlap the opposite (-0.2 or 0.2, respectively) threshold (Hopkins et al. 2009).

RESULTS: Many of the discrete force parameters estimated by both kinematic systems were in close agreement with the measured GRFs, with several effect sizes lower than 0.2 (Table 1). However, when estimated from the marker-based data, the vertical loading rate and peak vertical force during the running trials and vertical RFD during the CMJs were in poor agreement with those computed from the measured GRFs (ESs range: -0.86 to -0.30). Conversely, larger errors in the markerless system estimates of net horizontal impulse and peak horizontal force were observed during the running trials (ES = 0.67 and -0.96, respectively), and such differences were not present in the marker-based estimates.

Overall, for the CMJ trials, both the markerless and marker-based approach appeared to accurately estimate the vertical GRF (Figure 1), with mean RMSDs of 71.0 ± 66.8 and 78.5 ± 35.3 N, respectively (from onset of movement to the instant of take-off, after which RMSDs are much larger). Conversely, for the running trials, the marker-based estimates appeared to be more accurate overall compared with the markerless estimates. In fact, mean RMSDs for the vertical direction were 119.7 ± 32.5 and 150.5 ± 53.7 N, for the marker-based and markerless estimates, respectively, and 70.5 ± 24.7 and 121.9 ± 60.0 N, respectively, for the horizontal

direction. For additional context, these differences equate to between 4-5% of the peak vertical forces during CMJs, and 6-8% of the peak vertical forces and 35-42% of the peak horizontal forces measured during the running trials.

Table 1. Discrete force parameters (mean \pm SD) and the differences between measured and estimated values.

		Measured GRF	Estimated marker-based	Estimated markerless
CMJ	Peak vertical force (N)	1674.6 \pm 392.8	1651.2 \pm 358.4 [ES = 0.06 \pm 0.10]	1671.4 \pm 364.6 [ES = 0.01 \pm 0.10]
	Net vertical impulse (N·s)	164.7 \pm 39.7	171.4 \pm 38.9 [ES = -0.17 \pm 0.06]	164.0 \pm 38.3 [ES = 0.02 \pm 0.11]
	Vertical RFD (N·s ⁻¹)	9432.8 \pm 4883.5	10994.6 \pm 5669.3 [ES = -0.30 \pm 0.15]	10531.0 \pm 6761.4 [ES = -0.19 \pm 0.34]
Run	Peak vertical force (N)	1768.2 \pm 260.2	1887.6 \pm 292.5 [ES = -0.43 \pm 0.13]	1786.2 \pm 311.4 [ES = -0.06 \pm 0.16]
	Peak horizontal force (N)	200.8 \pm 49.2	193.7 \pm 48.3 [ES = 0.15 \pm 0.41]	287.0 \pm 130.8 [ES = -0.96 \pm 0.64]
	Net vertical impulse (N·s)	86.3 \pm 19.7	90.5 \pm 21.6 [ES = -0.20 \pm 0.08]	87.8 \pm 20.2 [ES = -0.08 \pm 0.08]
	Net horizontal impulse (N·s)	0.47 \pm 4.7	0.77 \pm 5.2 [ES = -0.06 \pm 0.30]	-2.69 \pm 4.7 [ES = 0.67 \pm 0.22]
	Vertical loading rate (N·s ⁻¹)	18185.5 \pm 4936.5	22731.1 \pm 5691.1 [ES = -0.86 \pm 0.32]	18912.4 \pm 4039.9 [ES = -0.16 \pm 0.42]

CMJ = countermovement jump; GRF = ground reaction force; RFD = rate of force development; ES = effect size \pm 90% CI. Bold ESs denote non-trivial differences between estimated and measured GRFs.

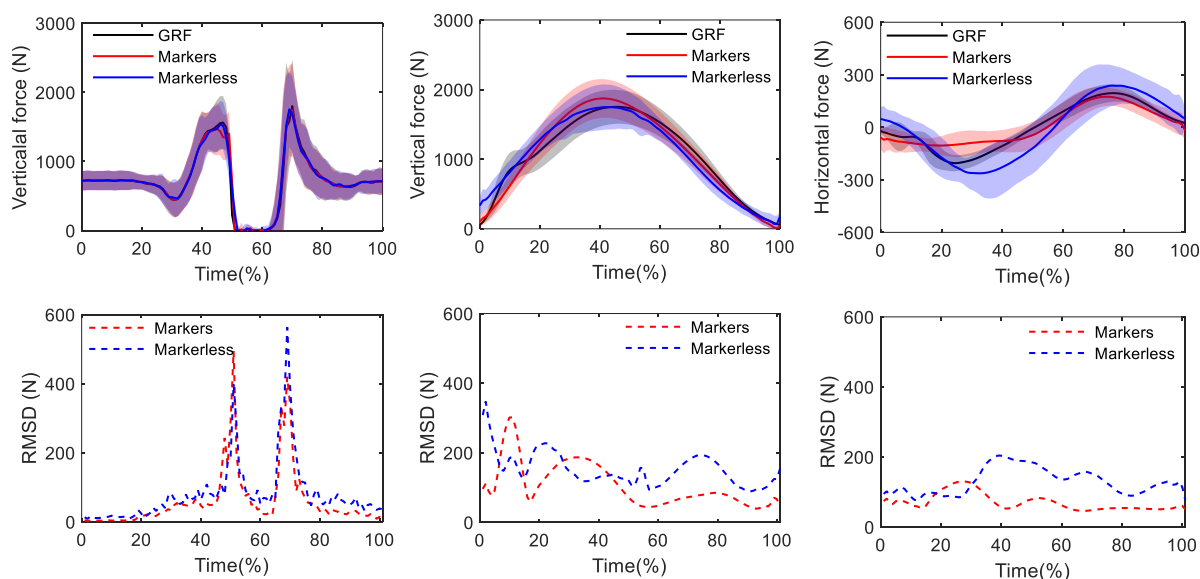


Figure 1: Mean (\pm SD) GRF waveforms (upper row) for all CMJ (left) and running (centre and right) trials, and the differences (lower row) between measured and estimated (marker-based and markerless) traces.

DISCUSSION: This study sought to investigate the ability of markerless motion capture to accurately estimate GRFs using an inverse (double differentiation of BCOM acceleration) approach through comparison with force-plate measured GRFs. Several discrete force parameters relevant to CMJ and running could be accurately estimated utilising either (marker-based or markerless) motion capture system. Specifically, the markerless system was able to accurately estimate vertical peak force, impulse and rate of development/loading during CMJ and running, in many cases more accurately than the marker-based system (Table 1). However, the marker-based system outperformed the markerless for the estimation of GRF

parameters in the horizontal direction. These findings build upon the study of Pavei et al. (2017) who showed marker-based motion analysis could accurately estimate several vertical GRF parameters relevant to running. However, here we show that many of these GRF outputs can be estimated with acceptable accuracy without the need for markers to be applied to the participant. This has the potential to open up opportunities for coaches and practitioners to more routinely track athletes' progress from either a performance (e.g. vertical impulse) or injury prevention (e.g. vertical loading rate) standpoint, outside of the laboratory in normal training situations. Furthermore, our markerless motion capture workflow could allow the estimation of vertical forces during running in the absence of an instrumented treadmill. For the CMJ and (for some applications) running, we consider the estimated instantaneous vertical force traces to be of an acceptable accuracy (RMSDs = 4-8% of the peak force; Figure 1). In fact, the observed errors are within the accuracy previously documented when resultant GRFs are estimated from whole-body segmental accelerations (RMSD = 2.48 N/kg; Verheul et al. 2019). On the contrary, the estimated instantaneous horizontal force traces are unlikely to be sufficiently accurate at this time, with much larger errors relative to the peak force measured (RMSD = 35-42%; Figure 1). Improved 2D pose estimation and the incorporation and optimisation of a Hertzian foot contact model into OpenSim (similar to Haralabidis et al., 2021) would likely improve the GRF estimates, however, more work is needed in this area to provide a widely applicable and computationally cheap solution. Additionally, future studies are required to understand the accuracy of these GRF estimations during other movements with more out-of-sagittal-plane motion and accelerations and/or decelerations, as marker-based GRF estimations have been shown to be poorer in these scenarios (Verheul et al. 2019).

CONCLUSION: Many GRF parameters of interest to sports practitioners can be estimated with sufficient accuracy from video alone and our markerless motion capture workflow. Although the computer vision system utilised in the current study is not yet widely accessible in the applied field, these findings do show initial promise for the accurate estimation of (particularly vertical) GRFs in field-based settings.

REFERENCES

- Cao, Z., Hidalgo, G., Simon, T., Wei, S-E & Sheikh, Y. (2017). Realtime multi-Person 2D pose estimation using part affinity fields. *IEEE Conference on CVPR*.
- Delp, S., Loan, J., Hoy, M., Zajac, F., Topp E. & Rosen, J. (1990). An interactive graphics-based model of the lower extremity to study orthopaedic surgical procedures, *IEEE Transactions on Biom. Eng.*, 37, 757-767.
- Haralabidis, N., Serrancoli, G., Colyer, S., Bezodis, I., Salo, A., Cazzola, D. (2021). Three-dimensional data-tracking simulations of sprinting using a direct collocation optimal control approach, *Peer J*, 9:e10975.
- Hopkins, W., Marshall, S., Batterham, A. & Hanin, J. (2009). Progressive statistics for studies in sports medicine and exercise science, *MSSE*, 41(1), 3-13.
- Johnson, C., Tenforde, A., Outerleys, J., Reilly, J. & Davis, I. (2020). Impact-related ground reaction forces are more strongly associated with some running injuries than others, *Am. J. Sp. Med.*, 48(12), 3072-3080.
- Morin, J-B, Bourdin, M., Edouard, P., Peyrot, N., Samozino, P. & Lacour, J-R. (2012). Mechanical determinants of 100-m sprint running performance, *Eur. J. App. Phys.*, 112(11), 3921-30.
- Needham, L., Evans, M. Wade, L., Cosker, D., McGuigan, P., Bilzon, J. & Colyer, S. (2022). The development and evaluation of a fully automated markerless motion capture workflow. *J. of Biomechanics*, 144.
- Pavei, G., Seminati, E., Storniollo, J. & Peyré-Tartaruga, L. (2017). Estimate of running ground reaction force parameters from motion analysis. *J of App. Biomechanics*, 33, 69-75.
- Verheul, J., Gregson, W., Lisboa, P., Vanrenterghem, J. & Robinson, M. (2019). Whole-body biomechanical load in running-based sports: The validity of estimating ground reaction forces from segmental acceleration. *J. of Sci. and Med. in Sp.*, 22(6), 716-22.

ACKNOWLEDGEMENTS: This research was funded by CAMERA, the RCUK Centre for the Analysis of Motion, Entertainment Research and Applications, EP/M023281/1 & EP/T014865/1